Received: Added at production | Revised: Added at production | Accepted: Added at production

DOI: xxx/xxxx

RESEARCH ARTICLE

On the Design and Implementation of Efficient Antennas for HF RFID Readers.

Ernest Ofosu Addo[1] | Benjamin Kommey*[2] | Andrew Selasi Agbemenu[2] | Hermann Kumbong[2]

[1]Department of Information Engineering and Mathematics, University of Siena, Siena, Italy

[2]Department of Computer Engineering, Kwame Nkrumah University of Science and Technology, Kumasi, Ghana

Correspondence
*Benjamin Kommey,
Department of Computer Engineering, Kwame Nkrumah University of Science and Technology, Kumasi, Ghana.
Email: bkommey.coe@knust.edu.gh

Abstract

This paper describes an in-depth methodical approach to the development of efficient high frequency (HF) antennas for usage in radio frequency identification (RFID) systems operating at 13.56MHz. It presents brief theory relevant to RFID communication and sets up a framework within which features and requirements of antennas are linked to key design parameters such as antenna form-factor and size; RF power level, materials and communication protocol. Tuning circuits necessary to adjust the resonance and power matching characteristics of antennas for good transponder interrogation and response recovery are discussed. To validate the approaches outlined, a complete step-wise antenna design and measurement described. Common practical problems that are often encountered in such design processes are also commented on.

KEYWORDS:
high frequency; RFID; antenna; tuning

1 | INTRODUCTION

According to many manufacturing, energy, and service industry experts, radio frequency identification has become arguably the most ubiquitous element for automatic identification and second only to the use of bar-coded labels, in the view of others [1,2]. Although the bar-code reading and other methods are still popular due to their low prices and/or longer market existence, the RFID technology has garnered a lot of interest since the turn of the millennium and its usage has been projected to see massive growth towards becoming the foremost identification method in this decade [3]. The widespread use of the RFID technology and its projected growth burst is mainly attributed to the technical optimally solutions it offers to the low data storage capacity and non-reprogrammability problems associated with the other identification methods [4]. The technology's popularity is also on account of its faster, more secure and hardier means of power and data transfer between a reader/interrogator and a tag located on/in a remote object of interest by the means of magnetic or electromagnetic (EM) waves. Owing to this principle of operation, RFID possesses the capability for non-line of sight and multiple object identification: two very important features required in applications like inventory control and automation.

RFID systems exist in many variants and can be differentiated by certain fundamental features. These include operation type, operating principle of data carrier, power supply, operating frequency range, and mode of data transfer. Based on the reader transmission frequency, RFID devices may be considered low frequency (LF): 30-300kHz, high frequency (HF): 3-30MHz, ultra-high frequency (UHF): 0.3-3GHz or microwave: >3GHz systems. The HF class of RFID devices operate generally at f_{op} =13.56 MHz (wavelength, $\lambda_{op} \approx$ 22m) in the ISM band and are able to achieve a read ranges up to 1m. Like most mainstream technologies, the operation of HF devices are regulated by various standards. These include the ISO 18000 set of general standards for RFID, ISO 14443 [5,6,7], ISO 15693 [8,9,10], and the EPCglobal Class 1 Gen 2. The standards define key radio interface parameters

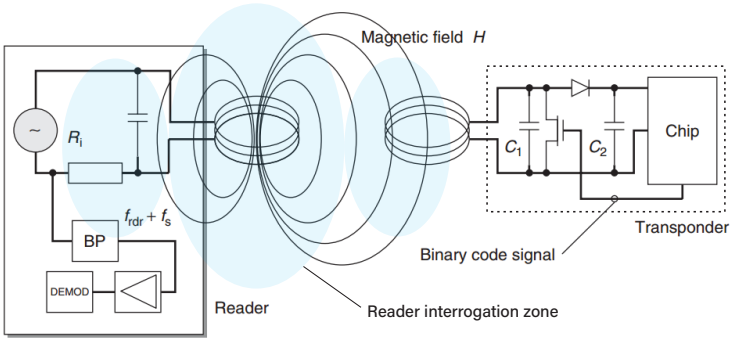

FIGURE 1 Operation of an HF-RFID system

such as modulation, subcarrier frequencies, bandwidth, and coding[11]. ISO 14443 compliant tags and readers are referred to as proximity integrated circuit cards (PICCs) and proximity coupling devices (PCDs) respectively. Similarly, vicinity integrated circuit cards (VICCs) and vicinity coupling devices (VCD) are nomenclature for devices based on the ISO 15693 standard.
In this paper, we present a methodical approach to designing efficient HF RFID interrogator antennas which guarantees good read ranges and sensitivity to tags. Several design considerations are outlined and practical implementations options are discussed. The paper extends this discussion and applies the techniques to an ISO 15693 system where an antenna is designed and prototyped for an industry standard reader as a means of validation.
This paper is organized as follows: Section 2 reviews some theory relevant to HF RFID communication. Next, key parameters and considerations for the design of an HF antenna are outlined in a comprehensive design flow in Section 3. The paper concludes with a validation in Section 4.

2 | HF RFID READER-TAG COMMUNICATION

HF RFID systems, like their LF counterparts, operate based on inductive magnetic coupling, as illustrated in Figure 1[5,8]. This sets up a two-way communication link between a reader and a passive tag and allows for power transfer to the tag in the interrogation zone of the reader which is the overlapped reactive near-fields of the two devices' antennas. Here, the readers antenna coil transmits a query by generating a strong amplitude modulated magnetic field. The time-varying field flux crosses the cross-section of the nearby tag antenna coil thereby inducing a voltage at the tag's antenna ports. This voltage is stepped-up in a resonant circuitry, rectified and serves as power supply for the tag chip. The draw on magnetic energy by the resonant tag creates feedback on the readers antenna which is often represented as a complex transformed impedance, Z_F at the reader's antenna coil given by Equation 1. Provided the mean dimensions of the antennas are small compared to λ_{op}, the reader-tag system could be represented by the equivalent lumped element model in Figure 2.

$$Z_F = \frac{(\omega_{op}\gamma(d))^2 L_t L_d}{Z_t + Z_{chip}}, \quad \gamma(d) \in [0, 1] \tag{1}$$

where $\omega_{op} = 2\pi f_{op}$ whiles Z_t and Z_{chip} are the tag antenna, and chip input impedances respectively. $\gamma(d)$ is the coupling coefficient which depends on the distance between the two antennas, d and their (equivalent) radii, r_t and r_d as stated in Equation 2, assuming that the two antenna coils are positioned parallel to each other and aligned on a common central axis; and provided $r_d \geq r_t$. Furthermore, it could be shown that $\gamma(d)$ is qualitatively related to the self inductances of the antennas, L_t and L_d; and their mutual inductance, M (Equation 2)[4,12].

$$\gamma(d) \approx \left(\frac{r_t r_d}{d^2 + r_d^2}\right)^{\frac{3}{2}} = \frac{M}{\sqrt{L_t L_d}} \tag{2}$$

In the tag, by switching a load (ohmic or capacitive) using data pulses in the tags circuitry, Z_F varies and voltage at the readers antenna output changes accordingly. This is called load modulation and it is used as a means by the remote tag to signal its unique identification or any other data to the reader as an answer to its query. In practical systems, this signaling isn't strong enough and hence not very distinguishable from the reader's significantly stronger signal. A more robust technique known as

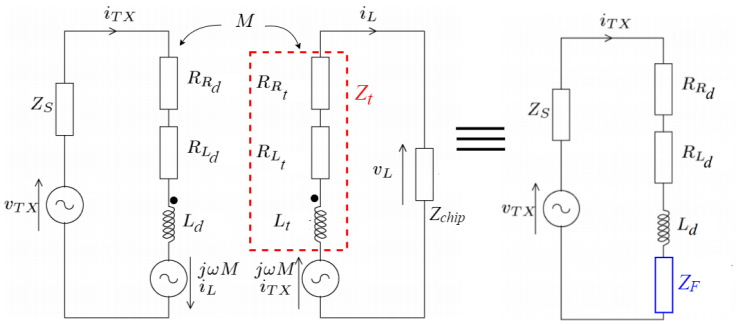

FIGURE 2 Near-field equivalent lumped element model showing the introduction of Z_F at the reader

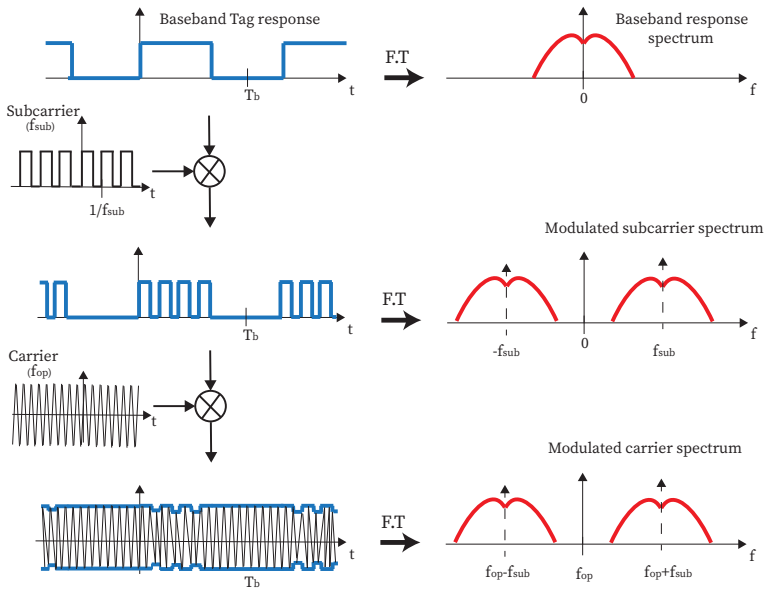

FIGURE 3 Load modulation of the baseband tag response with a subcarrier

load modulation with a subcarrier is often employed where the switching of additional load creates a new high elementary carrier at frequency, f_{sub} called a subcarrier. In 13.56 MHz systems, typical f_{sub} values include $f_{op} \times 2^{-n}$ where $n = 4, 5$, and 6. The subcarrier is first amplitude modulated in time with the data to be transmitted, creating two spectral lines at $\pm f_{sub}$. The modulated subcarrier is then used to modulate the carrier f_{op}. This shifts the two sidebands to frequencies $f_{op} \pm f_{sub}$. The data flow rides on these modulated sidebands which upon transfer, could be easily extracted, conditioned and demodulated at the reader's receiver front-end.

3 | ANTENNA DESIGN

3.1 | Design Considerations

Based on their operational principle, HF RFID antennas are typically designed as electrically small loops. Designing reader antennas for optimum performance requires knowledge of the complete RFID system's specifications such as reader front-end, antenna RF feed and possible tag characteristics. Since most systems operate at 13.56MHz, antennas are to be tuned to that frequency and have an impedance that matches the reader feed with a minimal reflection loss. Furthermore, when connected to the antenna, the reader must exhibit a very good frequency selectivity in order to capture tag responses. Another important design goal is the maximum read distance of tags, d_{max}. Since passive tag hardware depends on field launched by the reader for

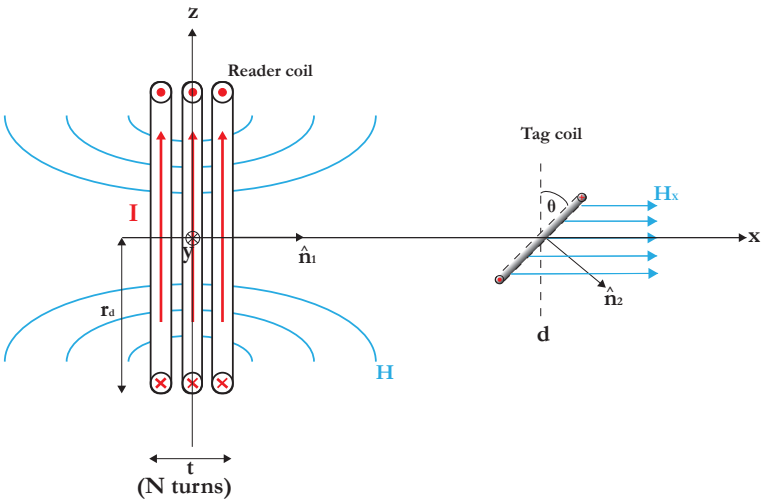

FIGURE 4 Loop antenna geometry and path of magnetic flux lines

power, the reader antenna must be designed such that the magnetic field (H_{min}) it produces at d_{max} is sufficient for both tag chip operation and RF communication. The transformer-type magnetic nature of the reader-tag coupling implies that d_{max} cannot be very large and that the read distance must be confined to the reactive near field of the antenna i.e. $d_{max} << \frac{\lambda_{op}}{2\pi}$. Indeed, the interrogation magnetic field H can be shown to attenuate rapidly beyond a certain distance with a decay of about 60dB per decade in free space[4]. Moreover, if the tag is located in the Fresnel or Fraunhofer region, it will receive a traveling wave instead of a quasi-static H field and the modifications to the field due to the presence of the tag will never be sensed by the reader. Such a quasi-static H field is guaranteed in the near field if the coil is supplied with a constant current.

3.1.1 | Form Factor and Sizing

Loop antennas are inexpensive, versatile and can take the form of numerous easily constructable shapes. They are typically poor radiators (see Equation 6) and are particularly suited for applications such as HF-RFID, where antenna radiation efficiency is not as important as the signal-to-noise ratio SNR and that systems do not depend on far-field radiation of EM waves for communication[13]. For short-range inductive radio links, the circular loop is often preferred as the current on the entire antenna is in phase and as such contribute constructively to the H field at a given distance d from the loop. Under the constant loop current assumption, the H field produced is found to achieve its largest strength at a certain ratio of the loop radius, r_d to d ($\xi = \frac{r_d}{d}$). That is, for every d_{max} specification, there exists an optimal r_d. Taking into account the phase difference along the total loop length, a compact cylindrical/circular antenna coil of radius r_d (i.e. total thickness, $t << r_d$) produces a magnetic field with component at an observation point X along the center line perpendicular to the coil's plane, $\vec{H}_x(d)$ with magnitude given by Equation 3 (refer to Figure 4).

$$\left|\vec{H}_x(d)\right| = \left| \int_0^D \frac{I\cos\theta e^{2\pi f_{op} l}}{4\pi(d^2 + r_d^2)} dl \right| = \frac{I r_d \sin(\frac{2\pi^2 d}{\lambda_{op}})}{4\pi^2\sqrt{(d^2 + r_d^2)^3}} \left| \sum_{n=0}^{N-1} e^{j\frac{4\pi^2 n r_d}{\lambda_{op}}} \right| \tag{3}$$

where $D = 2\pi r_d N$ is the total length of the loop material, N is the number of loop turns, I_l is the loop current amplitude and θ is the angle indicated in Figure 4. The optimal ξ value can be found by computing the limiting case, $d \to 0$, of the null-derivative condition for $\left|\vec{H}_x(d)\right|$ i.e. $\frac{\partial\left|\vec{H}_x(d)\right|}{\partial\xi} = 0$. An elaborate derivation of the general N case of this condition is performed in[14]. A simplified approach for the case of a single turn loop is shown in Equation 4.

$$\lim_{d\to 0} \frac{\lambda_{op}(2\xi^2 - 1)}{\xi} - \frac{2\pi^2 d(1+\xi^2)\sin(\frac{4\pi^2 r_d}{\lambda_{op}})}{1 - \cos(\frac{4\pi^2 r_d}{\lambda_{op}})} = 0 \tag{4}$$

The solution to Equation 4 shows that, for optimal performance, $r_d = \sqrt{2}d$ [13,15]. The result also holds for any given N. It should be noted that although a loop with radius $r_{d(opt)}$ is required for optimal performance of tags, an accurate assessment of a system's d_{max} requires knowledge of the minimum interrogation field strength, H_{min} of the tag to be used. That is the tag can still be sensed until a distance corresponding to the larger of the two intersection points root of the $\left|\vec{H}_x\right|$ vs r_d curve and the line $\left|\vec{H}_x\right| = H_{min}$ for a given current and number of turns. The derived condition suggests that longer read distances can be achieved by increasing the loop radius accordingly. However, this relationship is limited by the constant current precondition. The alternating current fed from the reader front-end can be assumed to be constant if D is small compared to λ_{op}. As a rule of thumb, the condition $D < 0.2\lambda_{op}$ is often used. Under this assumption, the static field strength at point d from Equation 3 can be simplified as shown in Equation 5 using the Biot-Savart law [16].

$$\left|\vec{H}_x(d)\right| = \left|\frac{NIr_d^2}{2\sqrt{(d^2 + r_d^2)^3}}\right| \tag{5}$$

When considering small loops with optimal radius, Equation 5 gives a notion that for a given current source, by taking more turns, the loop will produce a large H field at the tag position X. However, this is not necessarily true and the use of more loop turns becomes counter-productive even for moderately high N. With high N, the total loop length D becomes considerable with respect to λ_{op}. In such a case, there exists more current carrying conductor parts which contribute to the H field. These contributions are weaker due to the increased distance from these current carrying parts to point X hence the total field at the tag is very weak. Additionally, due to the phase differences along the larger loop, the contributions of all loop parts will be out of phase at X resulting in partial destructive interference, exacerbating the dip in field strength [14]. Furthermore, for D equal to $0.5\lambda_{op}$, or a multiple, standing wave effects are noticed. The loop experiences self-resonance, affecting the usability of the loop in the antenna set-up as the design of required current enhancing techniques (discussed in Section 3.2) is difficult and highly constrained. In cases like this, the antenna system will resonate at multiple frequencies and the energy will be divided amongst them [14,17]. It is noteworthy that if such enhancement techniques are employed, read distances d can be achieved with smaller radii r_d i.e $r_d < \sqrt{2}d$ since the feed current is amplified. The value of r_d would depend on the nature of the enhancement circuit but a conservative choice in such a case is $r_d \approx 0.5d$.

Power transferred in the antenna near-field region is predominantly inductive and tends to be more real as we move further away from the antenna. Hence, the antenna's reactive impedance of primary importance although its real part cannot be neglected. Provided the $D < \lambda_{op}$ condition is met, a loop antenna can be modeled fairly accurately with lumped components as shown in Figure 5. R_{RAD} is the radiation resistance which represents power launched as far-field electromagnetic waves. The real component of the loop conductor's internal impedance, due to phenomena like skin and proximity effects, is represented by the ohmic loss component R_{LOSS}. L is the loop inductance whiles the parasitic per unit-length capacitance between each pair of turns is quantified by C_p. For a loop made of solid wire with radius b, the radiation and ohmic resistances could be evaluated using Eqs. 6 and 7. The reactive quantities, L and C_p of such a loop are given in Eqs. 8 and 9 [18,19,20]. σ, μ, and ϵ are respective notations for the wire conductivity, magnetic permeability of medium and the electric permittivity of the wire insulation. In the absence of insulation, $\epsilon \rightarrow \epsilon_o = 8.85 \times 10^{-12}\text{F/m}$. It should be noted that equations for evaluating the lumped quantities may vary slightly depending on the shape of loop and the nature of materials used. As examples, expressions for square/rectangular loops are discussed in [13,18] and that for loops formed from hollow conductor tubes are given in [21].

$$R_{RAD} = 320N^2 \left(\frac{r_d}{\lambda_{op}}\right)^4 \pi^6 \tag{6}$$

$$R_{LOSS} = \frac{Nr_d}{b} R_s \left(\frac{R_p}{R_o} + 1\right) \tag{7}$$

$$L = N^2 \mu r_d \left(\ln\left[\frac{8r_d}{b}\right] - 2\right) \tag{8}$$

$$C_p = \frac{2\pi^2 r_d \epsilon}{\ln\left[\frac{t}{2bN} + \sqrt{\left(\frac{t}{2bN}\right)^2 - 1}\right]} \tag{9}$$

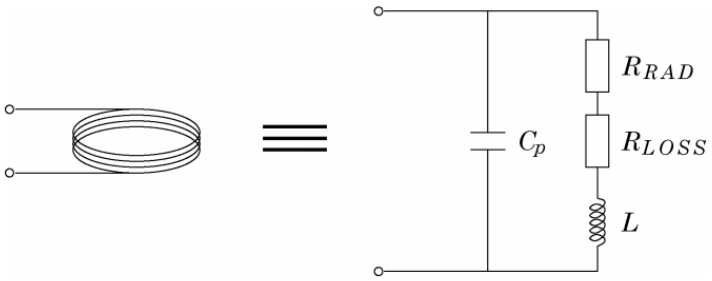

FIGURE 5 Equivalent lumped parameter circuit model of multiturn loop antenna

where $R_s = \sqrt{\frac{\omega_{op}\mu}{2\sigma}}$ is the surface impedance of the loop conductor, R_p denotes the per-unit length proximity effect ohmic resistance, and $R_o = \frac{NR_s}{2\pi b}$ is the per-unit length skin effect ohmic resistance. The ratio $\frac{R_p}{R_o}$ is discussed in [13] as a function of the ratio $\frac{c}{b}$ for loops with $2 \leq N \leq 8$ with $2c$ being the inter-turn spacing. In that analysis, it is shown that for close spacing ($\frac{c}{b} \to 1$), R_{LOSS} is twice as large as that in the absence of proximity effect i.e. $\frac{R_p}{R_o} = 0$.
From Eqs. 6 and 7, it is easy to infer that loop antennas are mostly lossy than radiative. Together, the resistance $R = R_{RAD} + R_{LOSS}$ is very small compared to the inductive impedance $\omega_{op}L$. To study the relation between loop's inductance and the strength of the H field it generates, the antenna is considered to be fed by a voltage source V_d in the reader front-end. From Equation 5, the H field generated is directly related to the magnetomotive force, MMF in the reader equivalent magnetic circuit. Discarding the small R and high impedance shunt loading of V_d by C_p; and employing Ampere's circuital law:

$$MMF = NI = N\frac{V_d}{\omega_{op}L} = N\frac{V_d}{\omega_{op}} \times \frac{S}{N^2} \propto \frac{V_d S}{N} \tag{10}$$

where S is the reluctance of the magnetic circuit and essentially represents the inverse of the inductance L' of single turn loop with the same cross sectional area. Therefore, affirming aforementioned sizing criteria to maximize $\left|\vec{H}_x(d)\right|$, it is best to use an optimally small size single turn loops made of large diameter wire i.e. $N = 1$ and small L'. Furthermore, by using the single turn loop, the problem of high R_{loss} due to proximity effect is eliminated. This is especially good for the communication properties of the RFID system. This is because the larger loop resistance translates to higher antenna thermal noise whose voltage spectral density is described by the Johnson-Nyquist formula ($\overline{v_n} = \sqrt{4kTR}$). Therefore in receive mode, though the signal level at the antenna output may be large, the SNR is poor and faint tag responses may be lost in the background noise. Additionally, with large (multi-loop) antennas, it is often difficult to meet legal transmitted power guidelines from regulatory bodies. According to the ETSI and FCC regulations, the maximum RF field generated by an antenna in Europe and the USA respectively must be limited to 4W ERP. Usually, larger loops are barely able to comply with this regulation and require extra special shielding to operate within this limit [22]. Other issues with large loops include the emergence of magnetic flux holes in the interrogation zone resulting in insensitivity to some tags and the very high loop L (Equation 8) which may make power matching very difficult to achieve.

3.1.2 | Construction Methods: Materials and Technologies

Each HF RFID application is unique and techniques used in realizing the reader antennas may vary from one use case to another. Loops are usually made from copper or aluminum although any conductive material could be utilized. However, the use of copper is often preferred due to its higher conductivity and availability. Moreover, aluminum poses challenges in construction processes like soldering and may require some special care, tools, or materials. Available methods of constructing HF loop antennas include wire (insulated or bare) [14,22], hollow tubes [14,23], conductor-backed adhesive tapes [22], PCB etching [23,24,25], and conductive ink printing [26,27]. Although very robust, tube antennas are often bulky, tough to work with for neat appearance (unless special material such as refrigeration tubing is employed) and may require complex and oft non-stable setups for tuning and current enhancement. Tape antennas, on the other hand, are very simple and less bulky but are not hardy and require some protection from environmental conditions. PCB antennas are neat and are mostly employed for miniature systems where the loop is typically interfaced with onboard single-chip transceivers such as the TI TRF79xxA series. With fully onboard modules,

the sizes of antennas must be controlled as a very large antenna may not be properly driven by the low output power reader chip (∼200mW at 5V). Thickness of substrate and distance between trace windings are key additional factors affecting the performance of PCB antennas. Very thin substrates could cause fluctuations in μ values and loose loop windings could decrease L[24]. However, it should be noted that how tight the windings can be is limited by the manufacturing process. Such antennas may be etched by an average skilled person and do not necessarily require industry-grade processes or equipment. However, etching PCB antennas involve the use of harmful materials such as ferric chloride acid, hence the manufacturing process should be carried out meticulously and with safety equipment. A relatively new technique for realizing HF loop antennas is printing with conductive inks like silver particle ink on paper or PET substrates. Despite the low cost and great design flexibility advantages of this method, printed antennas are plagued with reduced read performance (poor frequency selectivity and low SNR) and high Joule heating due to their commonly high DC resistance[28,29,30]. Wire antennas are typically preferred as they provide a good balance of the pros and cons discussed above.

3.1.3 | Environmental Influences

The setting in which the antenna would be used, as well as its final mechanical casing, if any, are key to antenna performance and hence should be considered carefully. The presence of any metal (including other antennas) in close proximity to the loop, dampens and decreases the loop L hence de-tuning the antenna. Additionally, eddy currents in the metal generates an opposing H field and lower sensitivity to tag response signals[31]. These phenomena degrade the antenna's read range performance and the minimum separation from metal for noticeable de-tuning effects, grows with the loop size. For unavoidable exposure to metal, ferrite backing could be employed. This is a technique where a ferrite sheet is introduced to screen the loop from metal thus limiting de-tuning effects and improving antenna performance. Generally, it is advised that antennas always be tuned in their final positions or enclosures to account for inductance changes caused by both the metal and ferrite sheet[24].

Radio noise is another classical influence on antenna performance. Depending on the levels, radio noise can severely reduce reader receiver performance and limits its read range. Thus, noise sources are to be identified by surveying the site, preferably before starting the antenna design. Indoor electronic appliances, industrial equipment, and broadcasting radios are common sources due to the unwanted radio emissions from their electrical oscillators employed[32]. Locating such interference at HF could be done using the approach in explained in[33]. The antenna must also be sufficiently shielded to lessen the effect of such noise.

3.2 | Tuning and Current Enhancement Network

Standards for HF RFID systems specify the minimum interrogation magnetic field strength, H_{min} to be produced by reader antennas for proper operation of tags i.e. to build up a high enough voltage to power up the tag hardware. The ISO-15693 specifies $H_{min} = 0.15\text{A/m}$ (rms) whiles the ISO-14443 standard recommends $H_{min} = 1.5\text{A/m}$ (rms). However, it should be noted that there are tags from some manufacturers that are designed to operate very well with less (eg. for NXP cards, $H_{min} = 0.09\text{A/m}$). Consider the design of a VCD for a read distance, $d = 0.6\text{m}$. Using the optimal radius criterion with Equation 5 yields Equation 11. With $R < \omega_{op}L$, the voltage to be applied to the reader antenna to achieve d is given in Equation 12 where I_{min} is the minimum rms current needed in the antenna for H_{min}. For a single turn loop with $L = 1.5\mu\text{H}$, $|V_d| \approx 60V$. Feeding the loop with such high voltage directly from the reader front-end is not practical, hence enhancement techniques are required. This can be done either actively with the aid of an amplifier (eg. Class E) or passively by means of an RLC circuit.

$$\left|\vec{H}_x\right| = \left|\frac{NIr_d^2}{2\sqrt{(d^2+r_d^2)^3}}\right| = \left|\frac{NI}{\sqrt{27}d}\right| \tag{11}$$

$$|V_d| \approx I_{min} \times \omega_{op}L = \left|\frac{\sqrt{27}\omega_{op}dH_{min}L}{N}\right| \tag{12}$$

The extent of enhancement is not unbounded. In a passive approach, this can quantified by the quality factor Q of the resonator. In the tag-to-reader communication, the modulated tag response is captured by the reader antenna and relayed to the receiver front-end for demodulation. The received signal is conditioned and the subcarrier signal in the spectrum sidebands are extracted. Although guaranteeing larger RF power for the loop antenna, a large $Q = \frac{f_{op}}{BW}$ results in narrower bandwidth BW which conflicts with the reader band-pass characteristics resulting in poor carrier-subcarrier separation. Furthermore, the reader becomes susceptible to ringing issues which could interfere with protocol parameters such as bit timing[34]. A good compromise is to

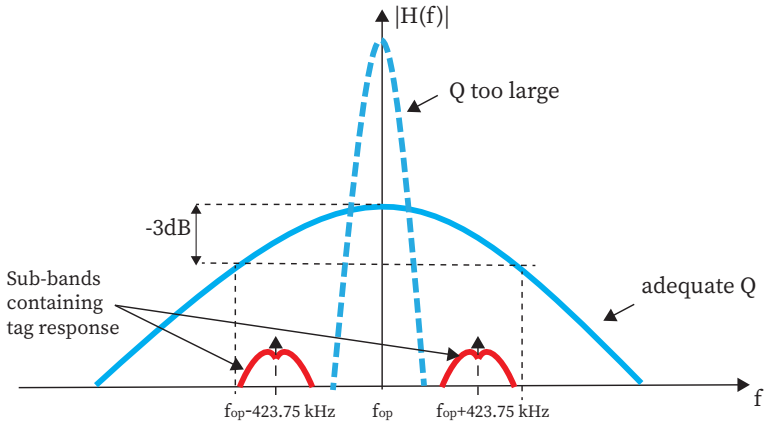

FIGURE 6 Band-pass characteristics observed for readers with adequate and very high Q antennas.

design for sufficient bandwidth allowing the undistorted reception of a modulated carrier signal whiles having enough power to meet the H_{min} criterion. For ISO 14443 applications, the standards prescribes a Q ranging between 6 - 10 and for ISO 15693 systems, the loaded antenna's Q must lie in the range of 15 - 20 for good performance (Figure 6)[8,5]. For an application that uses both standards, $Q = 7$ is recommended[24]. To enhance the current, the antenna must be made to behave as a parallel RLC circuit or slight variant of it. From Equation 9, it can be assumed that the impedance due to C_p is high enough at f_{op} hence the antenna is approximately a single time constant system whose dynamics are described by a large time constant $\tau = \frac{L}{R}$. Therefore, the unloaded quality factor of the antenna, $Q_o = \omega_{op}\tau$. The large Q_o could be reduced to an overall recommended value, Q_L by loading the antenna with a large shunt resistance R_{par} to produce an effective antiresonance with a lower quality factor $Q_{ext} = \frac{R_{par}}{\omega_{op}L}$. Since $R_{par} >> R$, it can be to proven that $Q_L = Q_o||Q_{ext} \approx Q_{ext}$. Therefore, in designing damping network, a desired Q_L is first selected and the appropriate shunt resistor value can be determined as $R_{par} \approx \omega_{op}LQ_L$. This resistance value could be fine-tuned for optimum performance. To achieve a parallel RLC chain which resonates at f_{op}, a (tunable) capacitance $C_{par} = \frac{1}{\omega_{op}^2 L}$ should be introduced into the network.

Lastly, the impedance of the loop antenna together with the enhancement and tuning networks should be matched to the reader feed. Typically, 50Ω coaxial (or shielded) cables are used to feed antennas to prevent undesired effects such as parasitic power emissions and power reflections which may arise due to the non-stationary nature of RF voltages at HF frequencies. To achieve power matching between the antenna and the reader output module via the coax supply, the damped antenna impedance $Z_{rd} = (R + j\omega_{op}L)||R_{par}$ must be transformed to $R_X = 50\Omega$. There are numerous techniques for matching antennas, some suitable for some construction technologies than others. Common methods include T-matching, gamma matching, and transformer matching. A technique which combines tuning, enhancement, and matching in a compact way is capacitance matching with damping. This technique is essentially an all-capacitor L-section since Z_d falls outside both unit resistance and conductance circles on the Smith Chart. Here, C_{par} is split into series and shunt elements C_1 and C_2 adding an extra degree of freedom to the network design. C_1 shifts Z_{rd} in the direction of the jX axis shown in Figure 7 (i.e. unto the unit conductance circle), while C_2 shifts the impedance point away from the origin in a circular path in the z plane (i.e. along the unit conductance circle to R_X). A simplified dimensioning of the shunt and series capacitance elements from C_{par}, R_X, and R_{par} are approximated in Eqs. 13 and 14 respectively. The values obtained for C_2 and C_1 are not exact and may need tuning. The circuit is then adapted to function as a balun to eliminate common mode noise, ringing and other effects due to the large voltage difference between the coax core and the outer grounded shield. Figure 8 shows the balanced version of the capacitance matching circuit.

$$C_2 \approx C_{par}\sqrt{\frac{R_{par}}{R_X}} \tag{13}$$

$$C_1 = \frac{C_2 C_{par}}{C_2 - C_{par}} \tag{14}$$

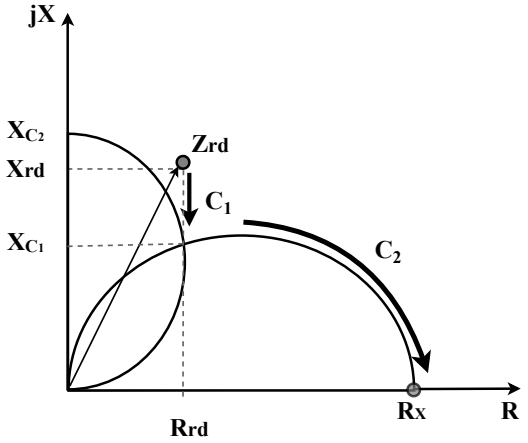

FIGURE 7 Z plane representation of Z_{rd} transformation by C_1 on C_2.

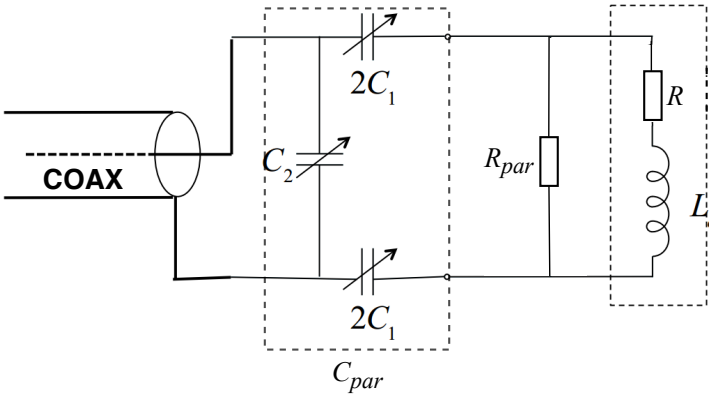

FIGURE 8 Circuit representation of damped loop antenna with a capacitance matching network

4 | VALIDATION AND CONCLUSION

A single turn circular loop HF antenna was designed, prototyped, and tested for read range $d_{max} = 0.6$m to validate the discussed methods and formulas. The loop of radius $r_d = 0.3$m was realized from a 1mm diameter copper wire (see Section 3.1.1). Using Eqs. 6, 7 and 8, the impedance of the antenna computed at f_{op} was $0.59 + j208.02\Omega$. The input impedance of the realized antenna (Figure 9) was determined by measuring the complex power reflection coefficient at the antenna port using the Agilent E5071c vector network analyzer. The measured input impedance of the antenna at f_{op} was $2.25 + j211.48\Omega$. The calculated and measured loop reactances bore close agreement. However, there was a discrepancy between the calculated and measured resistances which may be attributed to error in loop sizing and other sources of ohmic losses such imperfect contacts. The unloaded Q of the antenna coil was $Q_o \approx 94$, which was about five times the recommended limit. Designing for Q_L =18, a shunt resistor $R_{par} = \omega_{op} L Q_L \approx 3.80\text{k}\Omega$ was used as an initial design value. Capacitance matching was used to transform the damped antenna impedance to R_X. The resonance capacitance C_{par} was determined to be $\frac{1}{\omega_{op}^2 L} = 55.5$pF whiles C_2 and C_1 were 483.83pF and 60pF (Equation 13 and 14) respectively. The equivalent lumped element circuit of the antenna connected to a balanced capacitance matching network was simulated and tuned in the NI AWR Design Environment. The optimized damping and matching circuit parameter values were $R_{par} = 3.76\text{k}\Omega$, $C_1 = 62.50$pF, and $C_2 = 374.50$pF. The optimized antenna assembly resonates at 13.86MHz and has an input impedance, $Z_{in} = 50.34 - j0.0077\Omega$ at f_{op} achieving a simulated 50dB return loss at its input port when fed with a 50Ω source. The tuning and enhancement network was fabricated on PCB, connected to the antenna and tested as shown in Figure 10. It should be noted that in such a circuit, high rated components were used in order to withstand the high voltage that is generated in the resonant circuit. Furthermore, to deal with parasitics and ensure accuracy of circuit, adjustable components were introduced to allow the tuning of circuit after prototyping.

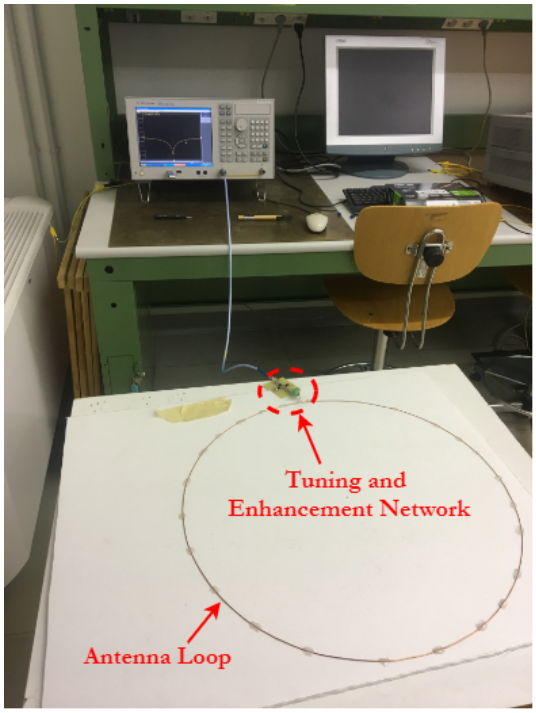

FIGURE 9 Impedance measurement and tuning of antenna prototype

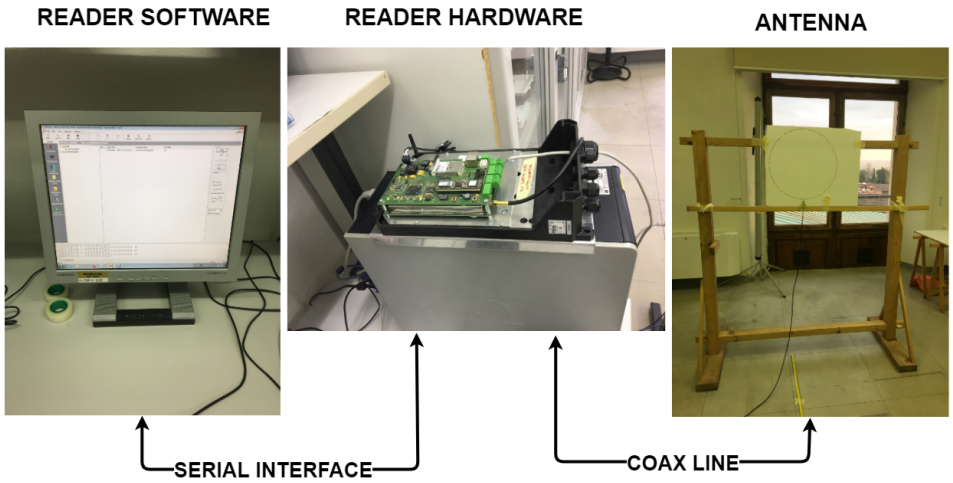

FIGURE 10 Read range test set-up

Using the OBID i-scan® ID ISC.2000-A as reader and NXP tags, read range measurements were performed to test the performance of the antenna. The RF energy supply was activated and the noise floor was measured to ensure that the amplitude of interference levels was low enough such that tag responses could easily be identified even at low signal levels. A low noise floor was also an indication of a good antenna matching circuit and test environment setup. The largest recorded d_{max} was 0.64m. From these measurement results, it can be concluded that the considerations, methods, and formulas discussed in this paper for the design of efficient loop antennas for HF RFID reader systems, are valid.

References

1. Wglarski M, Jankowski-Mihuowicz P, Chamera M, Dziedzic J, Kwanicki P. Designing Antennas for RFID Sensors in Monitoring Parameters of Photovoltaic Panels. *Micromachines* 2020; 11: 420. doi: 10.3390/mi11040420

2. Traub K. The GS1 EPCglobal Architecture Framework, GS1 a.i.s.b.l., v1.6. https://gs1.org/sites/default/files/docs/epc/architecture_1_6-framework-20140414.pdf; 2014 (accessed July 21, 2020).

3. Das R. RFID Forecasts, Players and Opportunities 20192029, Report, IDTechEx. https://www.idtechex.com/en/research-report/rfid-forecasts-players-and-opportunities-2019-2029/700; 2019 (accessed July 23, 2020).

4. Finkenzeller K. *RFID Handbook: Fundamentals and Applications in Contactless Smart Cards, Radio Frequency Identification and Near Field Communication*. Wiley Publishing. 3rd ed. 2010.

5. Cards and Security Devices for Personal Identification Contactless Proximity Objects Part 1: Physical Characteristics. standard, International Organization for Standardization; Geneva, CH: 2018.

6. Cards and Security Devices for Personal Identification Contactless Vicinity Objects Part 2: Air Interface and Initialization. standard, International Organization for Standardization; Geneva, CH: 2016.

7. Cards and Security Devices for Personal Identification Contactless Vicinity Objects Part 3: Anticollision and Transmission Protocol. standard, Geneva, CH: 2016.

8. Cards and Security Devices for Personal Identification Contactless Vicinity Objects Part 1: Physical Characteristics. standard, International Organization for Standardization; Geneva, CH: 2018.

9. Cards and Security Devices for Personal Identification Contactless Vicinity Objects Part 2: Air Interface and Initialization. standard, International Organization for Standardization; Geneva, CH: 2019.

10. Cards and Security Devices for Personal Identification Contactless Vicinity Objects Part 3: Anticollision and Transmission Protocol. standard, International Organization for Standardization; Geneva, CH: 2019.

11. Daki B, Damnjanovi M, ivanov L, Menianin A, Bla N, Kisi M. Design of RFID Antenna in Ink-Jet Printing Technology. In: . 1 of *2012 IEEE 10th Jubilee International Symposium on Intelligent Systems and Informatics*. ; 2012: 429-432.

12. Roz T, Fuentes V. Using Low Power Transponders and Tags for RFID Applications. *EM Microelectronic Marin* n.d: 1–8.

13. Balanis CA. *Antenna Theory: Analysis and Design*. Wiley-Interscience . 2005.

14. Aerts W, De Mulder E, Preneel B, Vandenbosch GAE, Verbauwhede I. Dependence of RFID Reader Antenna Design on Read Out Distance. *IEEE Transactions on Antennas and Propagation* 2008; 56(12): 3829-3837.

15. Lee Y. Antenna Circuit Design for RFID Applications. *Microchip Technology Inc.* 2003; AN70: 1-50.

16. Choudhury MH. *Electromagnetism*. J. W. Mason, Ed. Chichester and London, U.K.: Ellis Horwood . 1989.

17. Yates DC, Holmes AS, Burdett AJ. Optimal Transmission Frequency for Ultralow-Power Short-Range Radio Links. *IEEE Transactions on Circuits and Systems I: Regular Papers* 2004; 51(7): 1405-1413.

18. Stutzman WL, Thiele GA. *Antenna Theory and Design*. John Wiley Sons . 1998.

19. Magnusson P, Alexander G, Tripathi V, Weisshaar A. *Transmission Lines and Wave Propagation*. CRC Press . 2001.

20. Grandi G, Kazimierczuk M, Massarini A, Reggiani U. Stray Capacitance of Single-layer Solenoid Air-core Inductors. *IEEE Transactions on Industry Applications* 1999; 35: 1162 - 1168. doi: 10.1109/28.793378

21. Texas Instruments . HF Antenna Cookbook. *Technical Application Report* 2001; 11-08-28-001: 1–20.

22. Goulbourne A. HF Antenna Design Notes: Technical Application Report. Tech. Rep. SCBA034, Texas Instruments; 2015.

23. Kirschenbaum I, Wool A. How to Build a Low-Cost, Extended-Range RFID Skimmer. In: Proceedings of 15th USENIX Security Symposium. ; 2006: 43-57.

24. Jacobi R, LaCost E. Antenna Design Guide for the TRF79xxA: Application Report. Tech. Rep. SLOA241C, Texas Instruments; 2020.

25. Borja AL, Belenguer A, Cascon J, Kelly JR. A Reconfigurable Passive UHF Reader Loop Antenna for Near-Field and Far-Field RFID Applications. *IEEE Antennas and Wireless Propagation Letters* 2012; 11: 580-583.

26. Ailian C, Xianming Q, Zhi NC, Boon Keng L. Performance Assessment of Printed RFID Reader Antenna. In: 2007 IEEE Antennas and Propagation Society International Symposium. ; 2007: 301-304.

27. Xiao GG, Zhang Z, Lang S, Tao Y. Screen Printing RF Antennas. In: 2016 17th International Symposium on Antenna Technology and Applied Electromagnetics (ANTEM). ; 2016: 1-2.

28. Xiao G, Aflaki P, Lang S, et al. Printed UHF RFID Reader Antennas for Potential Retail Applications. *IEEE Journal of Radio Frequency Identification* 2018; 2(1): 31-37.

29. Koptioug A, Jonsson P, Sidén J, Olsson T, Gulliksson M. On the Behavior of Printed RFID Tag Antennas, using Conductive Paint. In: Antennas. ; 2003: 3.

30. Li X, Sidén J, Andersson H, Schön T. A Paper-Based Screen Printed HF RFID Reader Antenna System. *IEEE Journal of Radio Frequency Identification* 2018; 2(3): 118-126. doi: 10.1109/JRFID.2018.2869494

31. Petrariu A, Lavric A, Coca E. Design of an High Frequency RFID Multi-Loop Antenna for Applications in Metallic Environments. *Advances in Electrical and Computer Engineering* 2018; 18: 35-40.

32. Bianchi C, Meloni A. Natural and Man-made Terrestrial Electromagnetic Noise: An Outlook. *Annals of Geophysics* 2009; 50: 435–445. doi: 10.4401/ag-4425

33. Thompson T. Locating RF Interference at HF: A Proven and Practical Approach to Dealing with RFI from Grow Lights and More. *QST* 2014: 33–39.

34. Xiao G, Zhang Z, Fukutani H, Tao Y, Lang S. Improving the Q -Factor of Printed HF RFID Loop Antennas on Flexible Substrates by Condensing the Microstructures of Conductors. *IEEE Journal of Radio Frequency Identification* 2018; 2(2): 111-116.

How to cite this article: Addo E. O., Kommey B., Agbemenu A. S., and Kumbong H. (yyyy), On the Design and Implementation of Efficient Antennas for HF RFID Readers, *Engineering Reports*, *yyy;ss:pp–pp*.